Generation of 1.5-μm band time-bin entanglement using spontaneous fiber four-wave mixing and planar lightwave circuit interferometers

Hiroki Takesue*
NTT Basic Research Laboratories, NTT Corporation,
3-1 Morinosato Wakamiya, Atsugi, Kanagawa, 243-0198, Japan

Kyo Inoue
Department of Electrical, Electronics and Information Engineering,
Osaka University, 2-1 Yamadaoka, Suita, Osaka, 565-0871, Japan.

(Dated: February 1, 2008)

This paper reports 1.5-μm band time-bin entanglement generation. We employed a spontaneous four-wave mixing process in a dispersion shifted fiber, with which correlated photon pairs with very narrow bandwidths were generated efficiently. To observe two-photon interference, we used planar lightwave circuit based interferometers that were operated stably without feedback control. As a result, we obtained coincidence fringes with 99 % visibilities after subtracting accidental coincidences, and successfully distributed entangled photons over 20-km standard single-mode fiber without any deterioration in the quantum correlation.

PACS numbers: 42.50.Dv, 42.65.Lm, 03.67.Hk

arXiv:quant-ph/0508215v1 29 Aug 2005

In recent years, the generation and distribution of entangled photon pairs have been studied intensively with a view to realizing such forms of quantum communication as quantum cryptography [1, 2], quantum teleportation [3] and quantum repeaters [4]. Although practical entanglement sources based on parametric down conversion (PDC) have been reported and widely used in the short wavelength band [5, 6], what is needed most for scalable quantum communication networks over optical fiber is a practical entanglement source in the 1.5-μm band, where silica fiber has its minimum loss. Several polarization entanglement sources in the 1.5-μm band have already been reported [7, 8, 9, 10]. However, when transmitting polarization entangled photons over optical fiber, polarization mode dispersion (PMD) causes decoherence, which limits the transmission length. Therefore, polarization entanglement is not the best choice for quantum communication over optical fiber.

Time-bin entanglement has been proposed to overcome this problem [11]. This scheme is based on qubits spanned by two time slots instead of two polarization modes, and so is unaffected by PMD. Although degenerated photon pairs in the 1.3-μm band [11] and non-degenerated photon pairs in the 1.3/1.5-μm band [12] have been reported with this scheme, the use of photon pairs where both photons are in the 1.5-μm band is obviously the most effective way of increasing the transmission length. Recently, a Hong-Ou-Mandel experiment using quantum correlated photon pairs both in the 1.5-μm band was demonstrated by Halder et al. [13]. However, the direct observation of the degree of entanglement on time-bin entangled photons in the 1.5-μm band has yet to be achieved. The large bandwidths of the previous entangled photon-pair sources pose another problem. Although there have been a few reports on entangled photon-pair sources with narrow bandwidths [9, 13], most of the previous time-bin entanglement experiments employed PDC that generated photon pairs with a typical bandwidth of $\sim$10 nm [12]. This relatively large bandwidth made it difficult to distribute such photons over a standard single-mode fiber (SMF) with a zero dispersion wavelength of $\sim$1.3 μm, because of the pulse broadening caused by the large chromatic dispersion of the SMF. Since most installed fibers are standard SMF, a long-distance transmission capability over a standard SMF is an important requirement for the entangled photons for quantum communication utilizing existing fiber networks. Also, fiber interferometers have been used in previous experiments to observe two-photon interference. Such interferometers are unstable and need feedback control to ensure their long-term stability [12].

In this paper, we report a time-bin entanglement generation experiment, in which the degree of entanglement was directly measured for time-bin entangled photon pairs both in the 1.5-μm band. We employed the spontaneous four-wave mixing (SFWM) process in dispersion-shifted fiber (DSF) [8, 9], with which we obtained quantum correlated photon pairs with narrow bandwidths. To observe two-photon interference, we used 1-bit delay interferometers made of planar lightwave circuits (PLC), which are silica-based optical waveguides fabricated on silicon substrates [14]. The excellent stability of the PLC interferometers enabled long-term measurements to be performed without feedback control. As a result, we observed a coincidence fringe with 99 % visibility after subtracting accidental coincidences. Moreover, we successfully distributed the entangled photons over 20 km of standard SMF without any deterioration in the quantum correlation, thanks to the narrow bandwidths of the

*Electronic address: htakesue@will.brl.ntt.co.jp;

entangled photons.

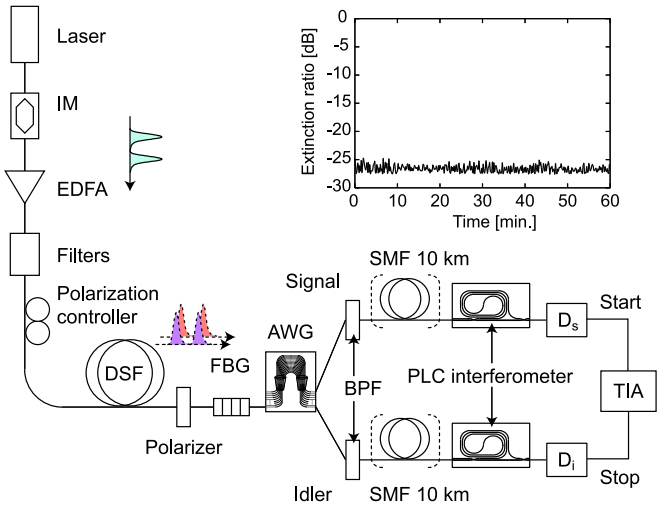

FIG. 1: Experimental setup and extinction ratio of PLC interferometer monitored for an hour.

Figure 1 shows the experimental setup. A continuous lightwave with a wavelength of 1551.11 nm from an external cavity semiconductor laser is modulated into double pulses with a 1-ns interval using an intensity modulator (IM). The pulse width and repetition frequency are 90 ps and 100 MHz, respectively. The coherence time of the laser output is $\sim$10 μs, which is far larger than the temporal interval between the pulses [15]. The double pulses are amplified by an erbium-doped fiber amplifier (EDFA), and filtered to reduce amplified spontaneous emission noise from the EDFA. The pulses are then input into a 2.5-km DSF with a zero-dispersion wavelength of 1551 nm after polarization adjustment. In the DSF, time-correlated photon pairs are generated through SFWM, with the double pulses as the pump. The pump, signal and idler frequencies, f_p, f_s and idler f_i, respectively, have the following relationship: $2f_p = f_s + f_i$. We set the pump power at a relatively small value so that the probability of both pulses generating photon pairs becomes very low. As a result, we can generate a time-bin entanglement, which is a superposition of two-photon states in different time instances expressed as

$$|\Phi\rangle = \frac{1}{\sqrt{2}}\left(|1\rangle_s|1\rangle_i + e^{i\phi}|2\rangle_s|2\rangle_i\right). \quad (1)$$

The expression $|k\rangle_x$ represents a state in which there is a photon in the kth time slot in a mode x, signal (s) or idler (i). ϕ is a relative phase term that is equal to $2\phi_p$, where ϕ_p is the phase difference between the two pump pulses. With pump degeneration, the efficiency of four-wave mixing in a long fiber reaches maximum when the pump, signal and idler photons are all in the same polarization state [16], so the correlated photons generated in the SFWM are expected to have the same polarization state as the pump photons. The phase matching condition of the SFWM is satisfied by setting the pump wavelength at the zero-dispersion wavelength of the DSF, as in our experiment. The use of longer fiber increases the efficiency of the SFWM process, by which we can increase photon pair production within the fixed bandwidths determined by the filters for separating signal and idler photons.

The output light from the DSF passes through a polarizer, whose function is explained later, and is input into fiber-Bragg gratings (FBG) to suppress the residual pump photons. Then, the photons are input into an arrayed waveguide grating (AWG), which separates the signal and idler photons. AWG output channels with peak frequencies of -400 and $+400$ GHz from the pump photon frequency are used for the signal and idler, respectively. The output photons from the AWG are filtered using dielectric bandpass filters (BPF) to further suppress the pump photons. With the FBGs, AWG and BPF, the transmittance of the pump photons becomes <-125 dB smaller than those of the signal and idler photons. The 3-dB bandwidths of the signal and idler channels are both 25 GHz ($\simeq$ 0.2 nm), which is very small compared with most previous photon-pair sources, and approximately 1/3 and 1/4 of the bandwidths of the narrowband photon-pair sources reported in [9] and [13], respectively.

The signal and idler photons are then input into PLC interferometers, which convert a state $|k\rangle_x$ to $\left(|k\rangle_x + e^{i\theta_x}|k+1\rangle_x\right)/\sqrt{2}$, where θ_x is the phase difference between the two paths of the interferometer for mode x, and can be tuned by changing the temperature. Then, after passing through the PLC interferometers, the state shown by Eq. (1) becomes

$$\begin{aligned}|\Phi\rangle \;\rightarrow\; & |1\rangle_s|1\rangle_i + (e^{i(\theta_s+\theta_i)} + e^{i\phi})|2\rangle_s|2\rangle_i \\ & + e^{i(\phi+\theta_s+\theta_i)}|3\rangle_s|3\rangle_i, \end{aligned} \quad (2)$$

where an amplitude term that is common to all product states is omitted for simplicity and non-coincident terms are discarded because they do not appear in a coincidence measurement. Thus, we can observe two-photon interference at the second time slot. The photons output from the PLC interferometers are input into photon detectors based on InGaAs avalanche photodiodes (APD) operated in a gated mode with a 4-MHz frequency [17]. By applying a 1-ns-wide gate only in the second time slots, we post-select the second term on the right hand side of Eq. (2). The quantum efficiencies of the detectors for the signal (D_s) and idler (D_i) were 8.0 and 9.5 %, respectively. The dark count rate per gate was 4 $\times 10^{-5}$ for D_s and 7.5 $\times 10^{-5}$ for D_i. Both PLC interferometers had a 2.0-dB loss. The signal and idler arm losses were 7.0 and 7.1 dB, respectively. The detection signals from D_s and D_i are input into a time-interval analyzer (TIA) as start and stop pulses, respectively, for the coincidence measurement.

In previous reports on SFWM, noise photons possibly due to spontaneous Raman scattering (SRS) were observed [18, 19], which degraded the visibility of the two-photon interference [8, 9]. SFWM photons have the same

polarization as the pump, while SRS photons are depolarized. Therefore, we can suppress the cross polarization component of SRS photons by placing a polarizer after the DSF as in Fig. 1 [18]. We adjusted the polarization of the pump photons with a polarization controller, so that we could maximize the ratio of the SFWM photon number to the SRS photon number.

We first measured the time-correlation of photon pairs without inserting PLC interferometers. We measured the coincidence rates at matched and un-matched slots, which we refer to as R_m and R_{um}, respectively. A coincidence in a matched slot is a "true" coincidence caused by photons generated with the same pump pulse. A coincidence in an un-matched slot corresponds to an accidental coincidence caused by photons generated by different pump pulses and it appears at different time instances separated by the detector gate period. Therefore, the ratio $C = R_m/R_{um}$ is a good figure of merit: $C > 1$ implies the existence of a time correlation. In our TIA measurement, C can be expressed as

$$C = \frac{R_m}{R_{um}} = \frac{\mu_c \alpha_s \alpha_i}{c_s c_i} + 1, \tag{3}$$

where μ_c, α_s and α_i show the average number of correlated photon pairs per pulse, the system transmittance (including detector quantum efficiency) for the signal, and that for the idler, respectively. c_s and c_i are the average count rate per pulse for the signal and idler, respectively, and can be expressed as

$$c_x = (\mu_c + \mu_{xn})\alpha_x + d_x \tag{4}$$

where $x = s, i$. Here, μ_{xn} and d_x are the average number of noise photons per pulse in mode x and the dark count rate for D_x. Using Eqs. (3) and (4), the experimentally obtained C, the system transmittances and the count rates, we can estimate the ratio between correlated and noise photons. We changed the average photon number per pulse by changing the pump power, and measured the coincidence rate. The squares in Fig. 2 show C as a function of the average number of idler photons per pulse $\mu_i (= \mu_c + \mu_{in})$. C reached 8.3 at an average idler photon number of 0.01. The circles and diamonds show the ratio of correlated photons for the signal and idler, respectively, which were calculated using Eq. (3). The signal was slightly noisier than the idler because of the slight difference in the SRS gain for the Stokes and anti-Stokes side. Although we can improve the portion of correlated photons as we increase the average number of photons, C degrades because the intrinsic accidental coincidences caused by the Poissonian statistics of the SFWM photons pairs increase. In the following two-photon interference experiment, we adopted $\mu_i = 0.13$, where the portion of correlated photons was ∼45 % and $C \simeq 4$.

We then measured the long-term stability of a PLC interferometer and the pump laser frequency. A continuous lightwave from the pump laser was input into a PLC interferometer. We adjusted the phase difference induced

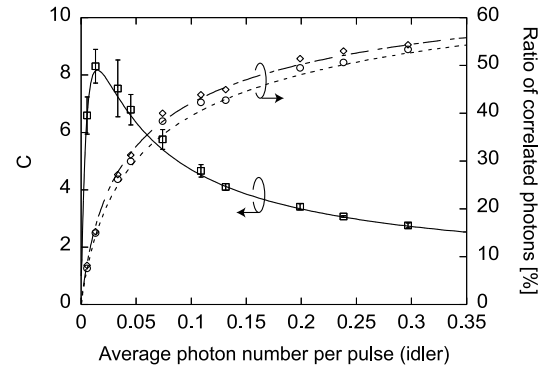

FIG. 2: C value and ratio of correlated photons as a function of average idler photon number. Fitted curves were produced based on the pump-power dependence functions of the number of correlated and noise photons obtained in the experiment.

in the two paths so that we could observe a dark fringe from one of the output ports. We monitored the extinction ratio, which is the ratio of the powers from the two output ports, for one hour. The result is shown in the top right in Fig. 1. The extinction ratio was better than -25 dB throughout the measurement. This means that we could operate our PLC interferometer and the pump laser stably for at least one hour without feedback control.

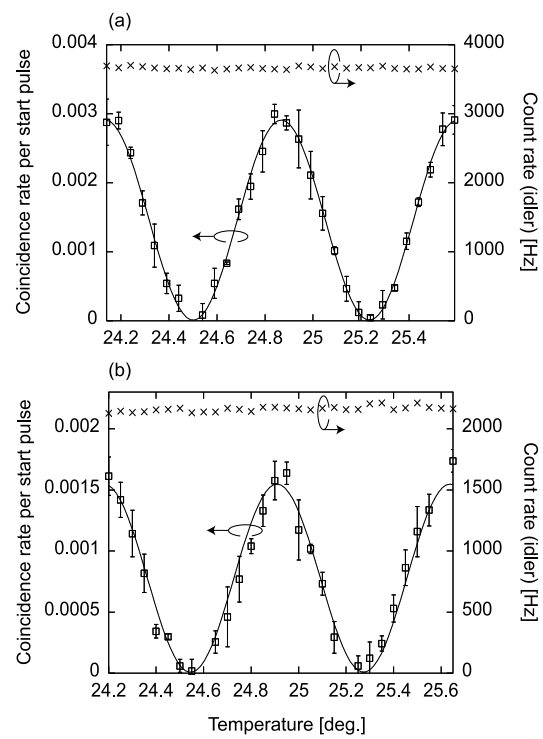

FIG. 3: (a) Coincidence rate per start pulse and count rate (idler) as a function of the temperature of the PLC interferometer for the idler. (b) After 10 km x 2 SMF transmission.

Next, we undertook a two-photon interference exper-

iment. We fixed the temperature of the PLC interferometer for the signal, changed that for the idler, and measured the coincidence. The peak power of the pump pulse was ∼80 mW and the average number of photons per pulse for both signal and idler was set at ~ 0.13. The coincidence rate per start pulse is shown by the squares in Fig. 3 (a), where accidental coincidences are subtracted. The count rate of D_s and the peak coincidence rate were ∼2800 and 4.5 Hz, respectively. While the count rate of D_i, shown by the x symbols in Fig. 3 (a), remained unchanged, we observed a deep modulation of the coincidence rate as we changed the temperature. The visibility of the fitted curve for the coincidence rate was as large as 99.3 %. When the accidental coincidences were included, the visibility was 61.4 %. The high extinction ratio and stability of the PLC interferometers contributed to this good visibility.

Finally, we inserted a 10-km standard SMF with a 1310-nm zero-dispersion wavelength in each path, and again measured the two-photon interference. The result is shown in Fig. 3 (b). Although the coincidence rate decreased due to the additional fiber loss of ∼2.3 dB for each path, the observed visibility remained at 99.0 % with the accidental coincidences subtracted. The visibility was 60.8 % with the accidental coincidences included. This result means that we observed no decoherence caused by SMF chromatic dispersion, and so the entangled photon source based on fiber SFWM is suitable for fiber transmission because it can generate photon pairs with narrow bandwidths.

In conclusion, we described the generation and observation of time-bin entanglement in the 1.5-μm band. SFWM in a DSF was used for the efficient generation of quantum-correlated photon pairs with narrow bandwidths. We used PLC interferometers, whose high extinction ratio and good stability made it possible to observe two-photon interference with a very high visibility of 99 %. A 20-km (10 km × 2) SMF transmission experiment was also undertaken and no degradation in visibility was observed thanks to the narrow bandwidths of the photon pairs. The excellent stability and long-distance transmission capability over standard SMF means that we can expect the above method to provide a practical entanglement source for quantum communication over optical fiber.

This work was supported in part by National Institute of Information and Communications Technology (NICT) of Japan.

[1] A. Ekert, Phys. Rev. Lett., **67**, 661 (1991).
[2] C. H. Bennett et al., Phys. Rev. Lett., **68**, 557 (1992). (1992).
[3] C. H. Bennett et al., Phys. Rev. Lett., **70**, 1895 (1993).
[4] H-J. Briegel et al., Phys. Rev. Lett., **81**, 5932 (1998).
[5] P. G. Kwiat et al., Phys. Rev. Lett., **75**, 4337 (1995).
[6] P. G. Kwiat et al., Phys. Rev. A, **60**, R773 (1999).
[7] A. Yoshizawa et al., Electron. Lett., **39**, 621 (2003).
[8] H. Takesue and K. Inoue, Phys. Rev. A, **70**, 031802(R) (2004).
[9] X. Li et al., Phys. Rev. Lett., **94**, 053601 (2005).
[10] H. Takesue et al., Opt. Lett., **30**, 293 (2005).
[11] J. Brendel et al., Phys. Rev. Lett., **82**, 2594 (1999).
[12] I. Marcikic et al., Phys. Rev. Lett., **93**, 180502 (2004).
[13] M. Halder et al., Phys. Rev. A, **71**, 042335 (2005).
[14] T. Honjo et al., Opt. Lett., **29**, 2797 (2004).
[15] The relative phase ϕ in Eq. (1) is equal to $2\Delta\phi_p$, where $\Delta\phi_p$ denotes the phase difference of the pump light between the first and second time slots [8]. This means that, if the coherence time of the pump is shorter than the temporal interval of these two slots, the relative phase ϕ is undetermined. Thus, the coherence time of the pump must be larger than the pulse interval in order to obtain an entangled pure state such as Eq. (1).
[16] K. Inoue, IEEE J. Quantum Electron., **28**, 883 (1992).
[17] An InGaAs APD for the long-wavelength band generally has a larger dark count probability than that of a Si-APD for the short-wavelength band. Therefore, to reduce noise counts, an InGaAs APD is normally biased above its breakdown voltage for a short period of time, which is called a gated mode operation. The upper limit of the gate frequency, which was 4 MHz in our experiment, is determined by the after-pulse characteristics of an APD.
[18] X. Li et al., Opt. Exp., **12**, 3737 (2004).
[19] K. Inoue and K. Shimizu, Jpn. J. Appl. Phys., **43**, 8048 (2004).